Int. J. Heat Mass Transfer. Vol. 20, pp. 919–926. Pergamon Press 1977. Printed in Great Britain

CONVECTION IN A VERTICAL SLOT FILLED WITH POROUS INSULATION

P. J. BURNS, L. C. CHOW and C. L. TIEN
Department of Mechanical Engineering, University of California, Berkeley, CA 94720, U.S.A.

(*Received* 16 *September* 1976 *and in revised form* 8 *November* 1976)

Abstract—Convective heat transfer through porous insulation in a vertical slot is examined analytically. A simple analytical formula for calculating the heat transfer is presented, after obtaining a matching coefficient by comparison with numerical solutions. Both free and forced convection, simulating wall leakage in common building structures, are considered. Numerical results for the case of no wall leakage are in good agreement with those presently available. It is shown that, for appreciable wall leakage, the dominant mode of heat transfer is due to the enthalpy change of the transferred fluid as it is blown through the enclosure.

NOMENCLATURE

A, aspect ratio, L/d;
d, horizontal distance between the hot and cold walls [m];
g, acceleration of gravity [m/s^2];
K_x, horizontal permeability [m^2];
K_y, vertical permeability [m^2];
L, vertical distance between the horizontal walls [m];
M, number of grid spaces in the horizontal direction;
n, non-dimensional coordinate normal to the boundary;
N, number of grid spaces in the vertical direction;
N_g, grid point about which the suction velocity is centered;
N_T, number of vertical temperature differences defined in equation (28);
Nu, Nusselt number defined in equation (7) or (8);
p, pressure [N/m^2];
Q_{cy}, non-dimensional heat transfer in the vertical direction defined in equation (20);
R_K, ratio of permeabilities, K_y/K_x;
Ra, modified Rayleigh number defined in equation (9);
Res, criterion for numerical convergence in equation (27);
T_h, hot boundary temperature [K];
T_{ho}, hot boundary temperature at $y = 0$ [K];
T_{co}, cold boundary temperature at $y = 0$ [K];
ΔT, temperature difference at $y = 0$, $(T_{ho} - T_{co})$[K];
$\bar{u}$, horizontal velocity [m/s];
u, non-dimensional horizontal velocity, $\bar{u}d/\alpha$;
U_w, non-dimensional horizontal blowing or suction velocity, u $(x = 0, 1; y)$;
$\bar{v}$, vertical velocity [m/s];
v, non-dimensional vertical velocity, $\bar{v}d/\alpha$;
V_w, non-dimensional vertical blowing or suction velocity, v $(x; y = 0, A)$;
$\bar{x}$, horizontal length coordinate [m];
x, non-dimensional horizontal length coordinate, $\bar{x}/d$;
$\bar{y}$, vertical length coordinate [m];
y, non-dimensional vertical length coordinate, $\bar{y}/d$.

Greek symbols

α, thermal diffusivity [m^2/s];
β, coefficient of cubical expansion [1/K];
γ, the fraction of the heat convected vertically that contributes to the Nusselt number as in equation (20);
θ, non-dimensional temperature difference, $(T - T_{co})/(T_{ho} - T_{co})$;
ν, kinematic viscosity [m^2/s];
ρ, density of the fluid [kg/m^3];
ρ_m, mean density of the fluid in the enclosure [kg/m^3];
τ, any non-dimensional numerical variable, either ϕ or Ψ, associated with equation (27);
ϕ, non-dimensional perturbation temperature defined in equation (26);
Ψ, non-dimensional stream function, $u = \dfrac{\partial \Psi}{\partial y}$ and $v = -\dfrac{\partial \Psi}{\partial x}$.

INTRODUCTION

THE FACT that fibrous materials are used as a universal building insulator renders them worthy of substantial evaluation. Even a slight improvement in the thermal effectiveness would exert a tremendous impact on overall energy consumption. Attention in this work is concentrated upon convective heat transfer through building insulation, although radiative heat transfer may also contribute to the total energy transport [1–3].

Both free and forced convection are important modes of heat transfer in ordinary building structure insulation. A two-dimensional vertical slot is taken as a basis for consideration, yielding results of fundamental as well as practical interest.

Recently, the subject of heat transfer in fiber insulations has received considerable attention. Free convection in insulation-filled enclosures has been the object of particular interest. While experimental results are available for a variety of configurations and insulation materials [4–9], there have also been several analytical studies [4, 6–8, 10, 11]. Bankvall [7] has been prolific in this area, and has presented a very complete literature survey.

Existing analytical studies are concerned primarily with very idealized physical systems, such as isothermal, impermeable boundaries, isotropic porous materials, etc. The present study was initiated to obtain realistic quantitative information and trends concerning convection phenomena in vertical insulation-filled slots as existing in building structures. The results will be of great practical importance to the building industry.

FORMULATION OF THE PROBLEM

Based on Darcy's law which is valid for the Reynolds number based on pore diameter being less than one, the governing differential equations are, in dimensional form [12]:

$$\frac{\partial(\rho\bar{u})}{\partial\bar{x}}+\frac{\partial(\rho\bar{v})}{\partial\bar{y}}=0 \tag{1}$$

$$\bar{u}=-\frac{K_x}{\mu}\frac{\partial p}{\partial\bar{x}} \tag{2}$$

$$\bar{v}=-\frac{K_y}{\mu}\left[\frac{\partial p}{\partial\bar{y}}+g(\rho-\rho_m)\right] \tag{3}$$

$$\bar{u}\frac{\partial T}{\partial\bar{x}}+\bar{v}\frac{\partial T}{\partial\bar{y}}=\alpha\left[\frac{\partial^2 T}{\partial\bar{x}^2}+\frac{\partial^2 T}{\partial\bar{y}^2}\right]. \tag{4}$$

The enclosure, shown in Fig. 1, is of height L and width d. The variables $\bar{x}$, $\bar{y}$, $\bar{u}$, $\bar{v}$ and T in equations (1)–(4) are non-dimensionalized as follows: $\bar{x}/d$, $\bar{y}/d$, $\bar{u}d/\alpha$, $\bar{v}d/\alpha$, and $(T-T_{co})/(T_{ho}-T_{co})$ to yield the un-barred quantities, x, y, u, v and θ, respectively. After invoking the Boussinesq approximation, introducing the stream function, and cross-differentiating the momentum equations to eliminate the pressure terms, the following equations, in non-dimensional variables, are obtained:

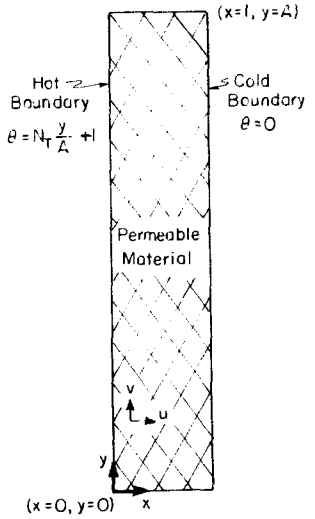

FIG. 1. Two-dimensional porous insulation-filled enclosure.

$$\frac{\partial^2\Psi}{\partial x^2}+\frac{K_y}{K_x}\frac{\partial^2\Psi}{\partial y^2}=-Ra\frac{\partial\theta}{\partial x} \tag{5}$$

$$\frac{\partial\Psi}{\partial y}\frac{\partial\theta}{\partial x}-\frac{\partial\Psi}{\partial x}\frac{\partial\theta}{\partial y}=\frac{\partial^2\theta}{\partial x^2}+\frac{\partial^2\theta}{\partial y^2}. \tag{6}$$

The associated boundary conditions are:

$$\Psi \text{ (boundaries): specified}$$

$$\theta \text{ or } \frac{\partial\theta}{\partial n}\text{ (boundaries): specified.}$$

The boundary conditions to be considered for equation (5) are: all boundaries impermeable resulting in a zero normal velocity at all walls, horizontal boundaries impermeable but the vertical boundaries are uniformly permeable yielding a uniform horizontal normal velocity at the walls: and horizontal boundaries impermeable but the vertical boundaries are locally permeable resulting in discrete mass injection (modeling the leakage due to cracks in the building structure walls).

The horizontal boundary conditions to be considered for equation (6) are: insulating boundaries, or perfectly conducting boundaries. The vertical boundary conditions are: isothermal walls, or non-isothermal walls. The only non-isothermal case to be discussed is a linear increase with height of the hot-boundary temperature. The left wall is the hot wall and acts as a source for induced motion.

The overall heat transfer is best characterized by the average Nusselt number for each wall of the enclosure, defined as follows:

$$Nu=\frac{1}{A}\int_0^A\left(U_w\theta-\frac{\partial\theta}{\partial x}\right)\mathrm{d}y \tag{7}$$

for the vertical walls [all of the Nusselt numbers reported herein are defined by equation (7)], or

$$Nu=\int_0^1\left(V_w\theta-\frac{\partial\theta}{\partial y}\right)\mathrm{d}x \tag{8}$$

for the horizontal walls. For no blowing, the Nusselt number reduces to an average non-dimensional temtemperature gradient at the wall, with a lower bound of one when conduction is the only mode of heat transport, and the vertical boundaries are isothermal.

The strength of convection is seen from equation (5) to be dependent upon the modified Rayleigh number, Ra. Explicitly,

$$Ra=\frac{g\beta(T_{ho}-T_{co})\,\mathrm{d}K_y}{\nu\alpha}. \tag{9}$$

For the onset of convection in vertical enclosures, a criterion of $Ra=4A$ was suggested [5], but this is not conclusively supported by experimental evidence. For

typical building insulation problems, $Ra \leqslant 100$. The permeability in the vertical direction, K_y, has been incorporated in the modified Rayleigh number as being more inductive of the flow for the large aspect ratios of current interest. For typical fibrous insulations, $10^{-10}\,\mathrm{m}^2 < K_y < 5\times10^{-8}\,\mathrm{m}^2$. Equation (9) implies that, for high aspect ratios, the fibers should be oriented perpendicular to the direction of the bulk flow so that the lower value of permeability will retard the flow to a greater extent. This is not generally done in present building structures. Fournier and Klarsfeld [5] indicate a typical value of two for the ratio of permeabilities, $R_K = K_y/K_x$, so the fiber planes should be rotated 90° to effectively utilize this difference. Wall leakage would decrease the utility of such a rotation.

The entire heat transfer through the porous insulation-filled enclosure may be characterized parametrically as:

$$Nu = Nu(Ra, A, R_K). \tag{10}$$

In general, Nu falls in the range of one to ten, and increases with the increase of Ra and the decrease of R_K. The dependence on A, however, is rather complicated.

ASYMPTOTIC SOLUTIONS FOR LARGE ASPECT RATIOS

A solution is sought that will indicate the effect of wall injection on the heat transfer phenomena in insulation-filled enclosures for large aspect ratios. It is reasonable to determine the solution for a fully developed flow in the vertical direction, which is the asymptotic case for large aspect ratios. A very approximate analysis similar to that of Batchelor [13] determines the range of validity of the asymptotic assumption to be $A > 0.1\,Ra$. Under this assumption, the equations reduce to:

$$\text{Continuity:}\ \frac{du}{dx} = 0 \tag{11}$$

$$\text{Momentum:}\ \frac{dv}{dx} = Ra\frac{d\theta}{dx} \tag{12}$$

$$\text{Energy:}\ u\frac{d\theta}{dx} = \frac{d^2\theta}{dx^2} \tag{13}$$

with the associated boundary conditions:

$$u(x = 0; 1; y) = U_w = \text{constant} \tag{14}$$

$$\int_0^1 v\,dx = 0 \tag{15}$$

$$\theta(x = 0, y) = 1;\ \theta(x = 1, y) = 0. \tag{16}$$

Solutions of the equations under these restrictions are:

$$u = U_w \tag{17}$$

$$v = Ra\left[\frac{e^{U_w x}}{1-e^{U_w}} + \frac{1}{U_w}\right] \tag{18}$$

$$\theta = \frac{e^{U_w x} - e^{U_w}}{1-e^{U_w}}. \tag{19}$$

Following Batchelor [13], it is reasoned that the heat convected in the vertical direction should influence the overall heat transfer by a factor, γ, such that the influence upon the Nusselt number of the heat convected vertically is:

$$\gamma Q_{cy} = \gamma\int_0^1 v\theta\,dx. \tag{20}$$

The factor, γ, is strictly dependent upon A, Ra and U_w, but may be taken as constant for the present range of these parameters.

This approach is expected to more closely model the enclosure with insulating horizontal boundaries than the one with perfectly conducting horizontal boundaries. The total heat transfer is due, then, to the heat conducted and convected in the horizontal direction, and the transport of heat in the upper and lower end regions due to the turning motion of the fluid traveling vertically which is given to within a factor by equation (20). The total Nusselt number may then be approximately given by:

$$Nu = U_w\frac{e^{U_w}}{e^{U_w}-1} + \gamma Ra\left[\frac{1+e^{U_w}}{2U_w(e^{U_w}-1)} - \frac{1}{U_w^2}\right]. \tag{21}$$

For the case of no blowing at the wall, equations (17)–(19), and (21), reduce to the following, respectively:

$$u = 0 \tag{22}$$

$$v = \frac{Ra}{2}(1-2x) \tag{23}$$

$$\theta = 1-x \tag{24}$$

$$Nu = 1+\gamma\frac{Ra}{12}. \tag{25}$$

Equations (21) and (25) indicate that, under the above assumptions, the average heat transfer is linearly dependent upon the modified Rayleigh number with the wall injection velocity, U_w, as a parameter. This result is substantiated by numerical computations, which indicate that the dependence is indeed a linear one for insulating horizontal boundaries and is at least approximately true for perfectly conducting horizontal boundaries.

Figure 2 depicts the variation of the Nusselt number with the wall injection velocity for modified Rayleigh numbers of 50 and 100. The horizontal boundaries are insulating. The discrete points are obtained by numerical calculation. The curves are graphical representations of equation (21) with a value of 0.055 for γ, obtained by fitting the curves to the discrete points. Agreement is excellent for positive values of U_w, but the curves tend to diverge from the points for large negative values of the abscissa. The asymptotic limit of the total heat transfer due to horizontal convection is shown. This limit is closely approached for values of U_w greater than 10 for the present range of Rayleigh numbers. Since all velocities are non-dimensionalized with respect to α/d, a typical value for which is about 2×10^{-4} m/s, the blowing is seen to exert an immense effect upon the total heat transfer. Physically, this is to be expected because typical free convection velocities are so small. Although a two-dimensional model for wall leakage is not physically realistic, the tremendous

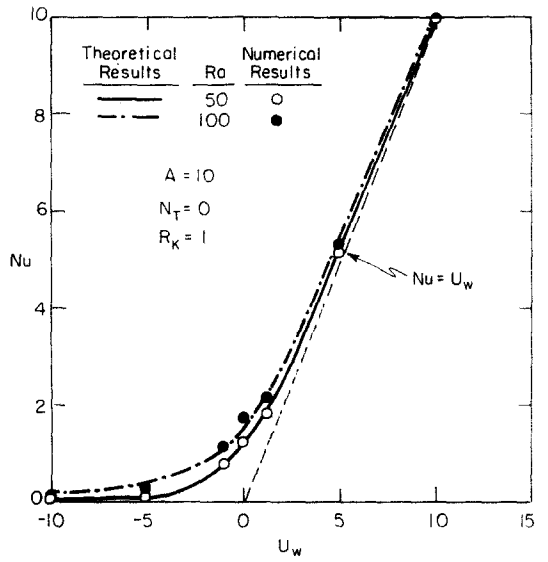

FIG. 2. Variation of the Nusselt number with the wall injection velocity.

impact of small leakage velocities has been illustrated. A uniform mass injection velocity over the entire cross-section is also not of practical interest. But, as a good first approximation, the heat transfer may be calculated as the enthalpy difference of the air on a mass flow basis, and the enhancement due to free convection may be added separately.

NUMERICAL RESULTS AND DISCUSSION

Equations (5) and (6) were put into a non-conservative central-difference form [14] and solved employing relaxation methods either on a CDC 6400 or a CDC 7600 computer. Instead of solving for the non-dimensional temperature, θ, the non-dimensional perturbation temperature due to convective motion, given by:

$$\phi = \theta - (1-x) \tag{26}$$

was solved for. This represents a more stringent criterion for convergence as well as decreasing the total number of iterations to achieve convergence.

The criterion set for convergence was:

$$\left(\frac{\tau_{new}-\tau_{old}}{\tau_{old}}\right)_{max} \leqslant Res \tag{27}$$

where τ refers to ϕ or Ψ, *Res* is a prescribed residue constant, and the subscript, max, denotes that the value in the parentheses is the maximum over all the grid points for both the energy and stream-function equations. An acceptable value for *Res* was determined to be 0.005 when the Nusselt number, defined by equation (7), did not change appreciably as *Res* was decreased to 0.001 and 0.0005. All of the numerical examples considered hereinafter are for insulating horizontal boundaries.

For the high aspect ratios considered, a grid ($M \times N$) of 8×16 was initially used. The grid spacing was reduced, on a step-by-step basis, to 16×16, 16×24 and 16×32. When the grid size was reduced, if the Nusselt number did not change by more than 2%, this was judged to be of sufficient accuracy such that the grid size need be reduced no further. This is not necessarily an adequate criterion for the convergence of the temperature and stream-function fields. Changes in the perturbation temperature of up to 20% were observed when the Nusselt number changed by about 5%. A four-point, one-sided difference was utilized in calculating the temperature gradient at the wall. The grid geometry is shown in Fig. 3.

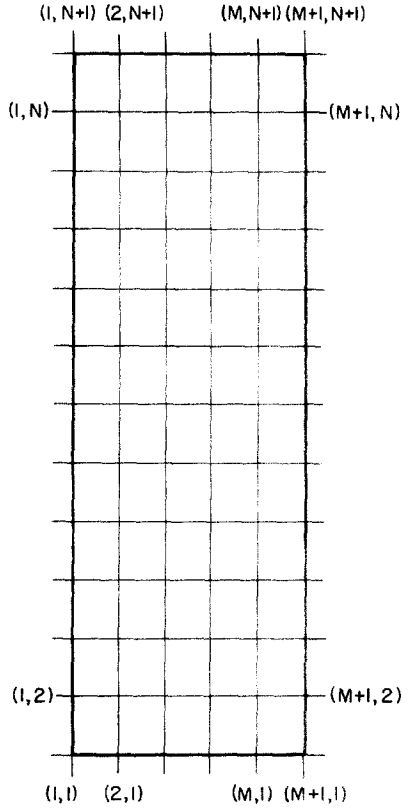

FIG. 3. Grid geometry.

For the cases with a high aspect ratio and ordinary boundary conditions (i.e. no blowing, suction, or boundary temperature gradients), a grid of 8×16 yielded sufficient accuracy. When the blowing and suction were uniform along the vertical walls, the grid was increased to 16×24, and when the blowing or suction occurred over discrete areas of the vertical walls, a grid of 16×32 yielded sufficiently accurate results. A grid of 24×64 was run for a case where the stability criterion [14] for the energy equation was violated in a few places. A negligible effect was observed. Results are judged to be accurate to 5%. For vertical temperature gradients on the hot boundary, a grid of 16×32 was employed, yielding results judged to be accurate to only about 15%. For low aspect ratios, grids of at least 16×16 were necessary. Table 1 presents some average values for the computer time used for different grids and numbers of iterations.

The variation of the Nusselt number with the aspect ratio is shown in Fig. 4 for Rayleigh numbers of 50

Table 1. Computer time used for calculations

Computer	No wall leakage Grid ($M \times N$)	Time (s)	Iter.	Uniform wall leakage Grid ($M \times N$)	Time (s)	Iter.	Discrete wall leakage Grid ($M \times N$)	Time (s)	Iter.
CDC 6400	8 × 16	10	151	8 × 16	4	48	8 × 16	6	102
CDC 6400				16 × 24	35	186			
CDC 6400				16 × 32	42	174	16 × 32	60	286
CDC 7600							16 × 32	5	325

Table 2. Numerical and asymptotic solutions for $A = 10$, $Ra = 50$ and no wall injection

x	$y/A = 0.250$			$y/A = 0.375$			$y/A = 0.500$			Asymptotic solution		
	u	v	θ	u	v	θ	u	v	θ	u	v	θ
0	0	25.9	1	0	25.1	1	0	25.0	1	0	25.0	1
0.250	0.03	12.0	0.721	0.01	12.4	0.745	0.01	12.5	0.750	0	12.5	0.750
0.500	−0.19	−4.79	0.472	−0.03	−0.07	0.496	0	0	0.500	0	0	0.500
0.750	−0.23	−12.2	0.236	−0.04	−12.5	0.248	0.01	−12.5	0.250	0	−12.5	0.250
1	0	−24.0	0	0	−24.8	0	0	−24.9	0	0	−25.0	0

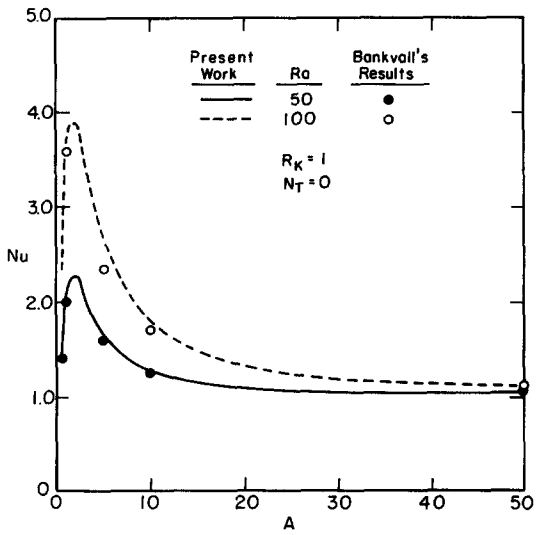

FIG. 4. Variation of the Nusselt number with the aspect ratio for impermeable vertical boundaries.

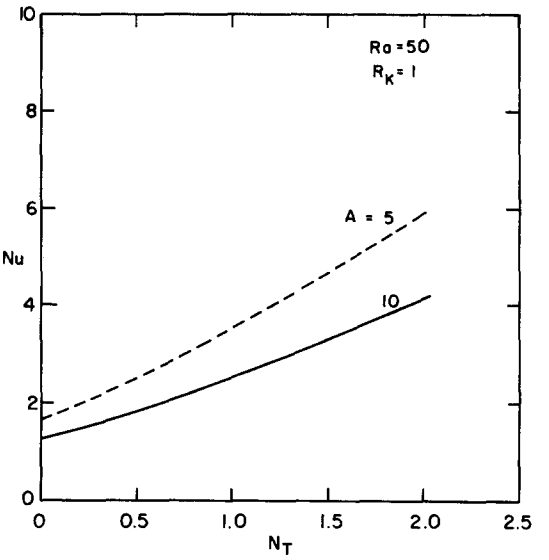

FIG. 5. Variation of the Nusselt number with the number of hot-boundary vertical temperature differences for no wall injection.

and 100. The discrete values are obtained from Bankvall [7] for purposes of comparison. Agreement is to within 5% for the entire domain of aspect ratios. For large aspect ratios, small horizontal temperature gradients exist on the upper region of the hot wall and the lower region of the cold wall, resulting in a decreased Nusselt number. For small aspect ratios, the fluid encounters much more flow resistance in the horizontal direction due to the increased path length. Thus, the curves undergo a maximum value near the aspect ratio of one.

Shown in Table 2 are some typical temperature and velocity values for an aspect ratio of ten. All of the profiles are anti-symmetric with respect to the center-point of the enclosure. The validity of the asymptotic solution is somewhat substantiated by the fact that the values obtained by numerical calculation do not differ greatly from the values obtained from the asymptotic solution, equations (22)–(24), except near the end regions, where the fluid undergoes a gross change in direction.

Figure 5 depicts the variation of the Nusselt number with N_T, the number of horizontal temperature differences at $y = 0$ which the hot boundary undergoes, defined by:

$$\theta(x = 0, y) = \frac{N_T}{A} y + 1.0. \tag{28}$$

The aspect ratio is a parameter, taking values of 5 and 10. The cold boundary is isothermal. A dramatic effect is observed due to the elimination of the small horizontal temperature gradients on the upper region

Table 3. Variation of the Nusselt number with the ratio of permeabilities for $A = 10$, $Ra = 50$ and no wall injection

R_K	0.1	0.5	1.0	2.0	5.0	7.5	10.0
Nu	1.29	1.28	1.27	1.25	1.22	1.20	1.18

Table 4. Numerical and asymptotic solutions for $A = 10$, $Ra = 50$ and $U_w = 5$

x	$y/A = 0.250$			$y/A = 0.375$			$y/A = 0.500$			Asymptotic solution		
	u	v	θ	u	v	θ	u	v	θ	u	v	θ
0	5	9.91	1	5	9.78	1	5	9.77	1	5	9.66	1
0.250	5.05	8.92	0.981	5.00	8.90	0.983	5.00	8.89	0.983	5	8.82	0.983
0.500	5.03	5.81	0.920	5.00	5.89	0.924	5.00	5.89	0.924	5	5.87	0.924
0.750	4.99	−4.50	0.716	5.00	−4.46	0.719	5.00	−4.45	0.719	5	−4.42	0.718
1	5	−40.3	0	5	−40.4	0	5	−40.4	0	5	−40.3	0

of the hot wall. The effect is more pronounced for the smaller aspect ratio because the wall undergoes a greater vertical temperature difference per unit of length. Results are estimated to be accurate to about 5% for $N_T = 0.5$ and only about 15% for $N_T = 2.0$.

The variation of the Nusselt number with the ratio of permeabilities, R_K, is shown in Table 3. Since the modified Rayleigh number is held constant, the variable, R_K, should be viewed as the variation of K_x. A typical value for R_K is two, which produces a negligible effect on the overall heat transfer. As mentioned before, the fiber planes should be rotated into a position such that they are perpendicular to the bulk flow.

Some typical temperature and velocity profiles for uniform wall injection as obtained by numerical calculation are presented in Table 4 along with the values obtained from the asymptotic solution with injection. The excellent agreement lends credence to the validity of the asymptotic solution. The only cases considered in this work are for a positive horizontal wall injection velocity (on the hot wall) and a positive wall suction velocity (on the cold wall). The horizontal boundaries are always impermeable.

Results will now be presented for a uniform injection velocity of $U_w = 5$ on the hot wall, and a constant suction velocity of 40 over one-eighth of the cold wall. The results are characterized by N_g, the grid point about which the suction velocity is centered. A grid of 16×32 was employed, so the suction velocity covers four grid spaces. Figure 6 presents the variation of the Nusselt number with N_g. When N_g is large, the forced flow tends to travel mainly with the natural flow, and when N_g is small, it travels mainly against the natural flow. For $N_g > 8$, the free and forced convection combine to increase the Nusselt number above the value obtained for uniform suction while for $N_g < 8$, the opposite effect is observed. A symmetrical effect is absent due to the slightly skewed nature of the flow because of the insulating horizontal boundaries.

The effect of a uniform injection velocity on the hot wall and a variable suction velocity on the cold wall will now be illustrated. The hot wall injection velocity

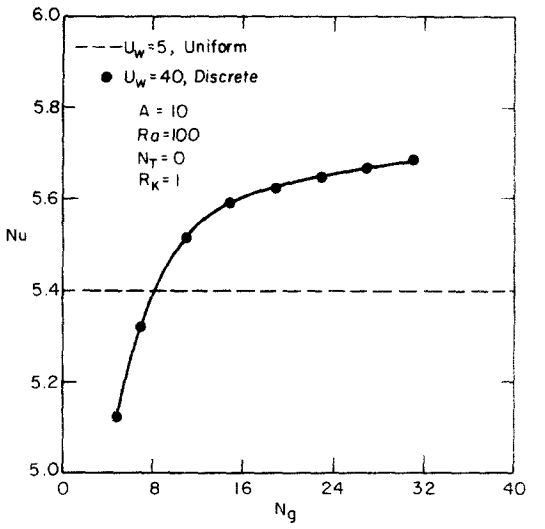

FIG. 6. Variation of the Nusselt number with the grid point about which the suction velocity is centered.

in all cases is $U_w = 5$. The mass is removed from the cold wall over the top one-eighth, one-quarter and one-half of the cold boundary and the bottom one-half, one-quarter and one-eighth of the cold boundary, resulting in suction velocities of $U_w = 40$, 20, 10, 10, 20 and 40, respectively. A grid of 16×32 was employed, so the mass is being removed from between the grid points 29–33, 25–33, 17–33, 1–17, 1–9 and 1–5, respectively. The variation of the Nusselt number with the suction velocity is presented in Fig. 7. Two curves are presented: one is for the removal on the lower portion of the cold wall; the other is for the removal on the upper portion of the cold wall. The curve for removal on the upper portion tends to increase the heat transfer above the value for uniform suction on the cold wall, while removal on the lower portion tends to decrease it due to the fact that the forced convection enforces and suppresses, respectively, the free convection.

To illustrate the effect of the interaction of the free and forced convection flow fields upon the total heat transfer, four cases are presented where the injection

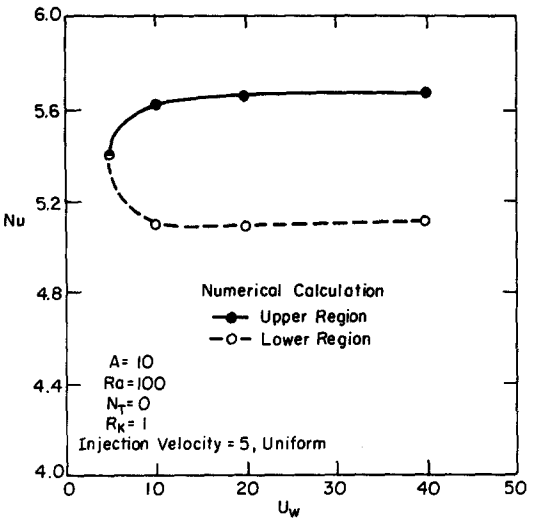

FIG. 7. Variation of the Nusselt number with the cold-wall suction velocity for suction on the upper and lower portion of the cold wall.

velocity through the hot wall is constant over one-eighth of the wall and zero over the rest of the wall, while the suction velocity through the cold wall is equal to the injection velocity and therefore possesses the same area of flow. In cases I and II, the fluid is injected through the bottom one-eighth of the hot wall, while in cases III and IV, it is injected through the top one-eighth of the hot wall. The fluid exits through the top one-eighth of the cold wall for cases I and III, and the bottom one-eighth for cases II and IV. A schematic diagram of the four cases is shown in Fig. 8. The Nusselt number when only free convection is present

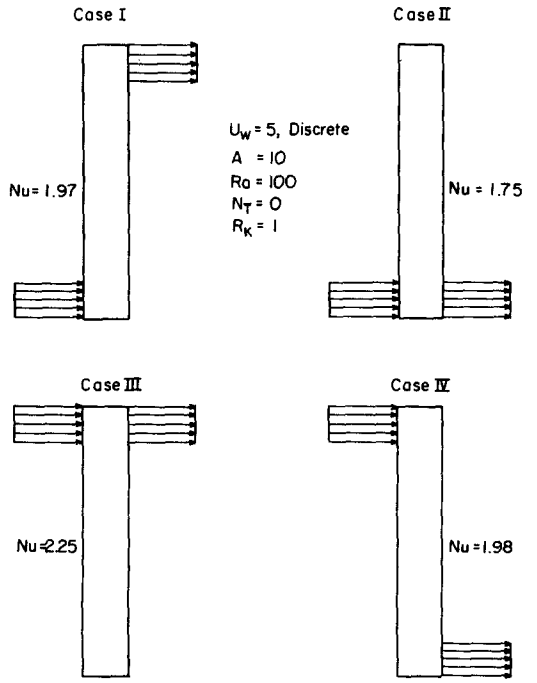

FIG. 8. Schematic representation of the four cases with discrete mass injection.

is 1.46. Case II acts to directly oppose the free convection, resulting in a low Nusselt number. Case III acts to directly augment the free convection, resulting in an increased Nusselt number. Cases I and IV act somewhere in-between, with about an equal effect upon the heat transfer. In all cases, the wall injection and suction velocities correspond to $U_w = 5$.

As was indicated before, free convection is not a strong mode of heat transfer. Any non-dimensional blowing velocities encountered in practice are likely to be huge, making this mode of heat transfer the dominant one. So, for three-dimensional enclosures, the heat transfer may be calculated, as a first approximation, as being due to the enthalpy change of the fluid being forced through the enclosure on a mass flow basis. If free convection is significant, it can be estimated and added to the forced convection and conduction.

CONCLUSIONS

In order to understand the heat-transfer process in common building walls, convective heat transfer through porous insulation in a vertical slot has been analytically examined. The results demonstrate the dependence of the Nusselt number on the Rayleigh number, aspect ratio, and anisotropic permeabilities. A simple, analytical formula for calculating the heat transfer has been developed after obtaining a matching coefficient by comparison with numerical solutions. The inadvisability of unfavorable boundary temperature gradients has been brought to light. Wall leakage, as simulated by mass injection and suction, has been shown to exert an imposing effect upon the heat transfer. Care must be taken to eliminate wall leakage in an area where the free convection would be enhanced. The fiber planes should be rotated so as to introduce the most flow resistance in the direction coincident with the bulk of the flow. Insulation should, perhaps, be self-contained in its own enclosure (i.e. a plastic wrap), as was done by Lopez [3], with at least one radiation shield. This would eliminate the problem of wall leakage and also allow the insulation to be arranged with the fiber planes oriented to oppose the bulk flow, with no opposing influence of cross flow.

Acknowledgement—This research was supported through a Grant on "Research on Building Insulation" by the Center for Building Technology, National Bureau of Standards (NBS). Many discussions with Dr. T. Kusuda of the NBS have been most helpful to the present work.

REFERENCES

1. J. D. Verschoor and P. Greebler, Heat transfer by gas conduction and radiation in fibrous insulation, *Trans. Am. Soc. Mech. Engrs* **74**, 962 (1952).
2. J. R. Mumaw, Variations of the thermal conductivity coefficient for fibrous insulation materials, M.S. Thesis, The Ohio State University (1968).
3. E. L. Lopez, Techniques for improving the thermal performance of low-density fibrous insulation, *Prog. Aeronaut. Astronaut.* **23**, 153 (1969).
4. C. G. Bankvall, Heat transfer in fibrous materials, *J. Testing Evaluation* **3**, 235 (1973).
5. D. Fournier and S. Klarsfeld, Some recent experimental data on glass fibre insulating materials and their use for a reliable design of insulations at low temperatures, ASTM STP 544, 223 (1974).

6. P. H. Holst and K. Aziz, A theoretical and experimental study of natural convection in a confined porous medium, *Can. J. Chem. Engng* **50**, 232 (1972).
7. C. G. Bankvall, Natural convective heat transfer in insulated structures, Lund Inst. of Tech. Report 38 (1972).
8. S. A. Bories and M. A. Combarnous, Natural convection in a sloping porous layer, *J. Fluid Mech.* **57**, 63 (1973).
9. T. Kaneko, M. F. Mohtadi and K. Aziz, An experimental study of natural convection in inclined porous media, *Int. J. Heat Mass Transfer* **17**, 485 (1974).
10. B. K. C. Chan, C. M. Ivey and J. M. Barry, Natural convection in enclosed porous media with rectangular boundaries, *J. Heat Transfer* **92**, 21 (1970).
11. J. E. Weber, Convection in a porous medium with horizontal and vertical temperature gradients, *Int. J. Heat Mass Transfer* **17**, 241 (1974).
12. M. Muskat, *The Flow of Homogeneous Fluids Through Porous Media*. J. W. Edwards, Michigan (1946).
13. G. K. Batchelor, Heat transfer by free convection across a closed cavity between vertical boundaries at different temperatures, *Q. Jl Appl. Math.* **12**, 209 (1954).
14. K. E. Torrance, Comparison of finite-difference computations of natural convection, *J. Res. Natn. Bur. Stand. B. Mathl Sci.* **72B**, 281 (1968).

CONVECTION DANS UNE LAME REMPLIE PAR UN ISOLANT POREUX

Résumé—On étudie analytiquement le transfert thermique par convection dans une lame d'un isolant poreux. On donne une formule simple de calcul du transfert thermique après avoir obtenu un coefficient d'adaptation par comparaison avec les solutions numériques. On considère à la fois les convections naturelle et forcée dans des cas qui simulent les structures usuelles des batiments. On montre que pour des fuites de paroi appréciables, le mode dominant du transfert thermique est dû au changement d'enthalpie du fluide transféré lorsqu'il est soufflé à travers l'ouverture.

KONVEKTION IN EINEM VERTIKALEN, MIT PORÖSER ISOLIERUNG GEFÜLLTEN SPALT

Zusammenfassung—Der konvektive Wärmeübergang in einem vertikalen, mit poröser Isolierung gefüllten Spalt wird analytisch untersucht. Es wird eine einfache analytische Beziehung zur Berechnung des Wärmeübergangs angegeben; die Anpassung an die numerische Lösung erfolgt mit Hilfe eines Koeffizienten. Es werden sowohl freie wie erzwungene Konvektion, welche die Wandleckagen in üblichen Baustrukturen simulieren, in Betracht gezogen. Numerische Ergebnisse für den Fall ohne Wandleckage sind in guter Übereinstimmung mit vorhandenen Resultaten. Es wird gezeigt, daß bei merklichen Wandleckagen der Wärmeübergang vor allem durch die Enthalpieänderung des durchströmenden Fluids bestimmt wird.

КОНВЕКЦИЯ В ВЕРТИКАЛЬНОЙ ЩЕЛИ, ЗАПОЛНЕННОЙ ПОРИСТЫМ ИЗОЛЯЦИОННЫМ МАТЕРИАЛОМ

Аннотация — Аналитически исследуется конвективный перенос тепла через пористый изоляционный материал в вертикальной щели. На основе численных решений выведена простая эмпирическая формула для расчета процесса переноса тепла. Рассматриваются как свободная, так и вынужденная конвекция, вызывающие утечку тепла в стенах строительных конструкций. Численные результаты для случая отсутствия утечки тепла хорошо согласуются с имеющимися данными. Показано, что при значительной утечке преобладает перенос тепла за счет изменения энтальпии переносимой жидкости по мере того, как она продувается через пористый материал.